Colloids and Surfaces A: Physicochem. Eng. Aspects 476 (2015) 83–89

Contents lists available at ScienceDirect

Colloids and Surfaces A: Physicochemical and Engineering Aspects

journal homepage: www.elsevier.com/locate/colsurfa

Regenerable Ag/graphene sorbent for elemental mercury capture at ambient temperature

Haomiao Xu, Zan Qu*, Wenjun Huang, Jian Mei, Wanmiao Chen, Songjian Zhao, Naiqiang Yan

School of Environmental Science and Engineering, Shanghai Jiao Tong University, Shanghai 200240, China

HIGHLIGHTS

- Ag/graphene composite was synthesized by a facile method.
- The Hg^0 capacity of Ag/graphene was 4.2 mg/g at ambient temperature (25 °C).
- The acid gases had no effect on Hg^0 removal efficiency.
- Mercury could be collected by thermal separation after adsorption.

GRAPHICAL ABSTRACT

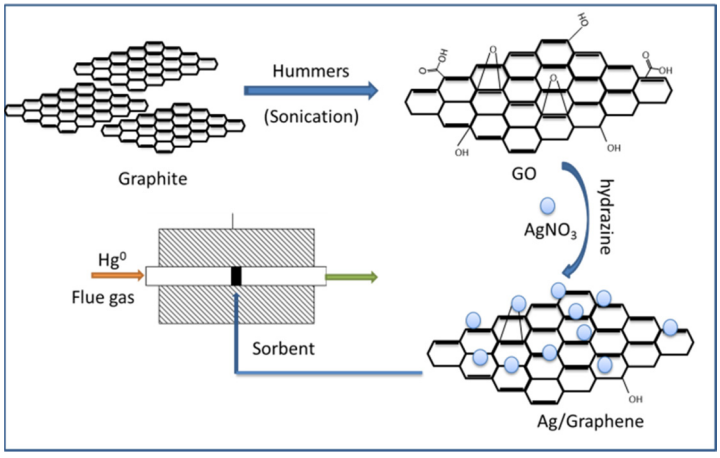

ARTICLE INFO

Article history:
Received 21 December 2014
Received in revised form 14 March 2015
Accepted 19 March 2015
Available online 27 March 2015

Keywords:
Graphene
Silver
Elemental mercury (Hg^0)
Adsorption

ABSTRACT

Elemental mercury (Hg^0) is a widespread concern due to its high toxic and long residence time in the environment. Ag/graphene composite was synthesized as a high efficient and recyclable sorbent for Hg^0 removal. Ag particles were doped on the surface of graphene by a facile in situ chemical synthesis method. FTIR, XRD, and TEM results showed that Ag nanoparticles successfully grew on the surface of graphene layers. The performance of Ag/graphene as a sorbent was tested under a fix-bed reactor and the results showed that it could completely capture Hg^0 at ambient temperature (25 °C). The Hg^0 capacity was as high as 4.2 mg/g. The Hg^0 removal efficiency decreased from 94% to 60% when the temperature increased from 25 to 100 °C, respectively. SO_2 and NO had nearly no effect on Hg^0 removal, but the efficiency dropped by about 4% when O_2 existed. Hg-TPD results showed that mercury can be rapidly and efficiently released from the composite by thermal separation. The adsorption capacity of Hg^0 had no degradation after six cycles. The high Hg^0 capacity and recyclability make the Ag/graphene a candidate for the removal at ambient temperature.

1. Introduction

Mercury has long been known to be toxic to humans [1]. After decades of hard work, the *Minamata Convention* was adopted in October of 2013, and it is a treaty aimed at controlling the mercury

* Corresponding author. Tel.: +86 21 54745591; fax: +86 21 54745591.
E-mail address: quzan@sjtu.edu.cn (Z. Qu).

http://dx.doi.org/10.1016/j.colsurfa.2015.03.027
0927-7757/

emission globally. The convention is expected to take effect in 2016, and it will call for a ban on the emission of mercury in 2018. The strict requirements about mercury control had been published by many countries. Therefore, it is significant to adjust and improve existing technologies or use the add-on technology to meet the new requirements.

In general, mercury is a trace element the environment, it existed stably in the fossil fuels such as coal and metal ores. But large amounts of mercury were transported from the geosphere into the atmosphere and hydrosphere through human activities in recent 200 years. It was reported that mercury emission from anthropogenic emissions greatly exceed natural geogenic sources, approximately 2100 tons of mercury is emitted by human activities annually [2]. Mercury emission from fuel combustion, waste incineration and mining are the main sources, resulting in high background level of mercury in the environment. And, more remarkable, elemental mercury (Hg^0) is one form of mercury, which is very hard to remove. It mainly exists in the atmosphere and the residence time of Hg^0 is several months to years [3]. Coal-fired power plants are regard as the largest emission sources. Hg^0 emission from coal-fired flue gas accounts approximately 35% of the total [3]. After coal-fired power plants, mercury emissions from cement and mineral production are the second largest anthropogenic sources [4,5]. Most of previous studies put more attention on the technologies for Hg^0 control among these major anthropogenic emissions. But mercury, as one kind of important resource, also exists in many artificial products (e.g., battery, thermometer, lamp, dental amalgam, and some electron devices). It was estimated that fluorescent lamp contain 0.72–115 mg of Hg per lamp, 500 mg for a typical fever thermometer [6,7]. In general, Hg^0 evaporated slowly from these broken products under ambient conditions. For these Hg-containing products, most of them were discarded with a low recycle rate. A large amount of mercury released from these products. The data showed that more than 14.1 tons of Hg^0 released into the environment from wasted batteries and fluorescent lamp annually [8].

Mercury is not only a pollutant but also an important resource. The future technologies for Hg^0 control should consider the high removal efficiency, the innocuity treatment and the recycling of resource. Adsorption method for the capture of Hg^0 was a potential technology. The mechanism for capturing Hg^0 over a sorbent can be divided into three sorts: amalgamation, physical adsorption and chemical adsorption [4,9–11]. Up to now, carbon, metals, metal oxides and selenium were often used as the Hg^0 sorbent at low temperature. Activated carbon (AC) was an efficient sorbent support due to its large surface areas and porosity. Sulfur modified AC showed the Hg^0 capacity of 2.6 mg/g at 20 °C along with the surface areas of 1000–1100 m^2/g [7,12]. But it is hard to recover the mercury from the sorbent because of the strong interaction between sulfur and mercury. Selenium was also an efficient sorbent for Hg^0 at low temperature. But this sorbent was not widely used because the toxic of selenium. Metal and metal oxides (e.g., CoO_x, MnO_x, FeO_x) are potential sorbents for the removal of Hg^0 at high temperature, they lose the activity for Hg^0 at low temperature. Furthermore, the mercury-contaminated sorbent in the environment could cause mercury secondary pollution. There is a strong motivation to develop a low-cost and recyclable sorbent for Hg^0 capture. The mechanism of Ag amalgamation exhibits good re-generation characteristic for Hg^0 capture. Silver doped on magnetic zeolite nanoparticles were efficient and recyclable sorbent for Hg^0 [13]. Carbon nanotube–silver composite was also synthesized for Hg^0 capture as a novel carbon-based sorbent, Ag was the main active site for Hg^0 adsorption [14]. A new approach for a recyclable sorbent was used by graphene. Graphene is single-atom-thick sheet of carbon first systematically isolated from crystalline graphite in 2004 [15]. Graphene, is currently, the most thinnest, strongest and stiffest material. Given the excellent in-plane mechanical, structural, thermal, and electrical properties of graphene, it have huge potential application in many fields [16] [17]. Graphene-based materials was used as a barriers for mercury vapor, which exhibit excellent performance for mercury vapor emission [18]. As a new member of the carbon family, there is still no attempt of the Ag/graphene based materials for the removal Hg^0. The large surface areas make it possible as a good supporter for Ag particles.

In our study, Ag/graphene composite was synthesized by a facile method and used it as a sorbent for Hg^0. The Hg^0 removal performance was evaluated in a fix-bed reactor. FTIR, XRD, and TEM were employed for the physiochemical characterization of Ag/graphene. We focus on the Hg^0 capture performance and the property of the sorbent's regeneration. The effect of adsorption temperature and different gases were also tested for optimizing the work condition.

2. Experimental

2.1. Sorbent preparation

Graphite oxide was prepared using Hummers method as described elsewhere [19]. In a typical synthesis method, 2 g of graphite and 1 g of $NaNO_3$ were added into 50 mL of 98% H_2SO_4, followed by stirring for 1 h. After that, 0.3 g of $KMnO_4$ was introduced into the mixture and kept stirring for 30 min. Then another 7 g of $KMnO_4$ was slowly added into the above mixture in 1 h. During this period, the temperature of the solution was kept below 5 °C by ice bath. Subsequently, the solution was heated to 35–40 °C and kept stirring for 2 h. After that, 90 mL of water was slowly added into the above solution in 15 min. Finally, 50 mL of water and 7 mL of H_2O_2 were added into the as-prepared solution, following by an obvious color change from brown to yellow. The above mixture was then filtrated and washed by 10% HCl and deionized water for several times. The product was kept drying at 80 °C for 48 h to give graphite oxide. Two hundred milligrams graphite oxide was added into 250 mL deionized water. Ammonia was used to adjust the solution's pH, the value was about 7.0. Then the above mixture was operated under ultrasonic for 1 h using high-speed stirring for 1 h to give graphene oxide (GO).

Two hundred milligrams of $AgNO_3$ was dissolved in 15 mL of ethyl alcohol with 5 mL of H_2O. This solution was then added into GO and kept stirring for 10 h. A mount of hydrazine hydrate was added and the mixture was kept at 90 °C for 12 h. When this reduction reaction was finished, the product was filtrated and dried in an oven at 100 °C for 5 h. After that, the solid product was transferred to a muffle furnace and calcined at 250 °C for 5 h. Fig. 1 shows the synthesis process of Ag/graphene.

2.2. Sorbent characterization

Powder X-Ray diffraction (XRD) (APLX-DUO, BRUKER, Germany) was used for the detection of the crystal structure of the as-prepared samples. The scanning range was from 10° to 80° with scanning velocity of 5°/min by using Cu-Kα radiation. The microstructure of the sorbent was analyzed by transmission electronic microscopy (TEM), and TEM image was performed on a JEOLJEM-2010 TEM device. The micrographs were obtained in the bright-field imaging mode at an acceleration voltage of 200 kV. The measurement of FTIR spectroscopy was carried out to characterize the surface properties. The N_2 sorption measurement was performed using Nova-2200 e, and the specific surface area was calculated using the Brunauer–Emmett–Teller (BET) method.

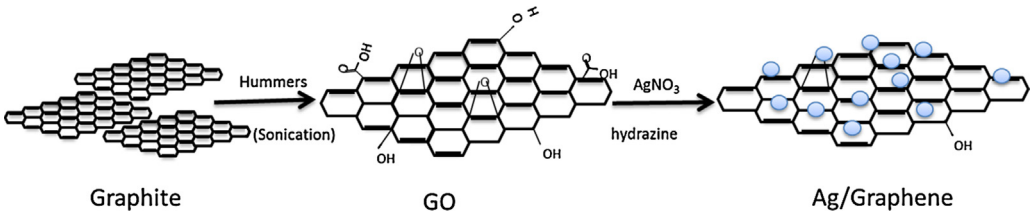

Fig. 1. The synthesis process of Ag/graphene.

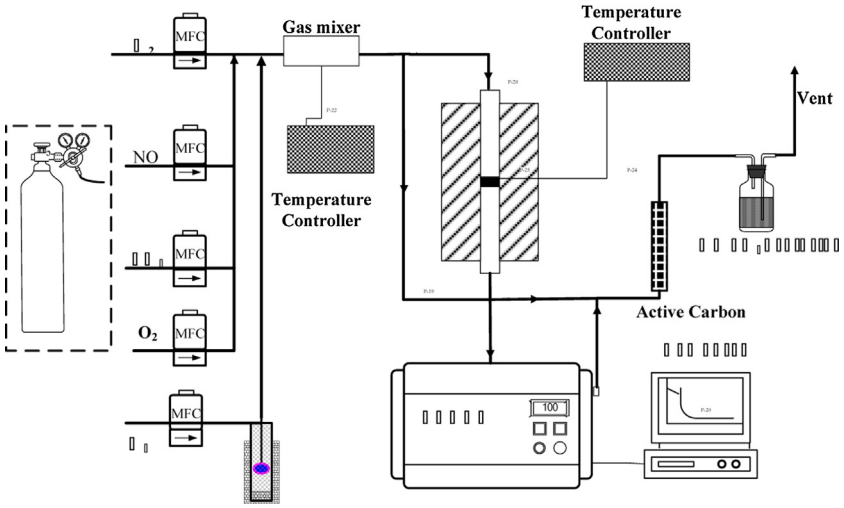

Fig. 2. The process flow of the assessment system.

2.3. Elemental mercury (Hg^0) capture

The Hg^0 adsorption performance of the prepared samples was evaluated in a fix-bed reactor. The process flow of the assessment system is sketched in Fig. 2. The experimental facility consists of a mercury permeation tube, a fixed-bed reactor, a cold vapor atomic absorption spectrometer (CVAAS) and an online data acquisition system. The Hg^0 concentrations of the influent and effluent were continuously measured by a CVAAS (SG 921, Jiang fen Ltd., China), which was calibrated by Lumex RA 915+ mercury analyzer. The temperature control device was employed to keep the reactor at the desired temperatures. The adsorption conditions were set as follows: a precisely weighted 30 mg of the samples; 0.5 mg/m^3 of Hg^0 generated from mercury permeation tube balanced in N_2 with a total gas flow rate of 500 mL/min. To test the effect of temperature on Hg^0 adsorption performance, the experiments were carried out at temperature range from ambient temperature (25 °C) to 100 °C. The adsorption time for each sample was about 100 min. The effect of different gases on Hg^0 capture was investigated, 4% O_2, 500 ppm SO_2, 500 ppm NO, or their mixture were introduced the simulated gas with a total flow rate of 500 mL/min balanced with N_2.

The Hg^0 adsorption capacity was calculated according the equation as follows:

$$Q = \frac{1}{m}\int_{t2}^{t1}\left(Hg^0_{in} - Hg^0_{out}\right) \times f \times dt$$

where Q is the Hg^0 adsorption capacity, m is the mass of sorbent in the fixed-bed, f denotes the flow rate of the influent, and t_1 and t_2 represent the initial and ending test time of the breakthrough curves, respectively.

2.4. Sorbent recycling

2.4.1. Hg-TPD

An Hg-temperature program desorption (Hg-TPD) method was built to test the desorption characteristics of Ag/graphene. After mercury adsorption at 25 °C for 100 min, the sorbents were regenerated by heating from 50 to 450 °C in a pure N_2 carrier gas. The heating rate was 2 °C/min with a flow rate of 500 mL/min of pure N_2.

2.4.2. Sorbent regeneration

After a fixed-bed reactor cooled down to the room temperature, another cycle of the Hg^0 adsorption test started. Six cycles of adsorption–desorption–adsorption were tested in our study.

3. Results and discussion

3.1. Sorbent characterization

3.1.1. FTIR

FTIR spectra were employed to analyze of functional groups of the as-prepared materials. For comparison, FTIR spectra of graphite, GO, and Ag/graphene were collected. As shown in Fig. 3, in the spectrum of graphite, there were no obvious peaks detected. For GO, the peaks observed at 1650 and 1548 cm^{-1} for GO were attributed to carboxyl C=O and C—O groups, respectively [20]. The peak at about 1130 cm^{-1} was attributed to epoxy C—O—C groups, and the peak at 1040 cm^{-1} was attributed to alkoxy C—OH groups. It was believed that the graphite was oxidized successfully by our oxidation method. In contrast, these bands were almost entirely absent in the spectra of Ag/graphene. The two well-defined peaks at 2850 and 2919 cm^{-1} were corresponded to epoxy CH_2 groups. GO was reduced by hydrazine hydrate in the reduction process. Moreover, there was no Ag–O peak at about 3450 cm^{-1} detected. It was

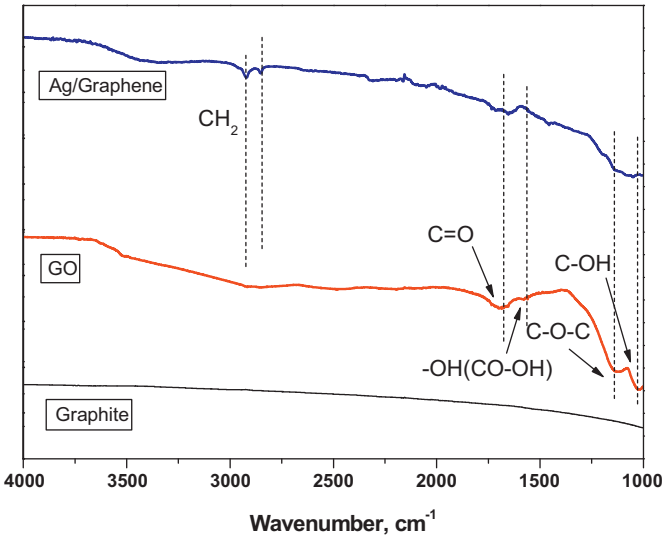

Fig. 3. FTIR spectra of graphite, GO, and Ag/graphene.

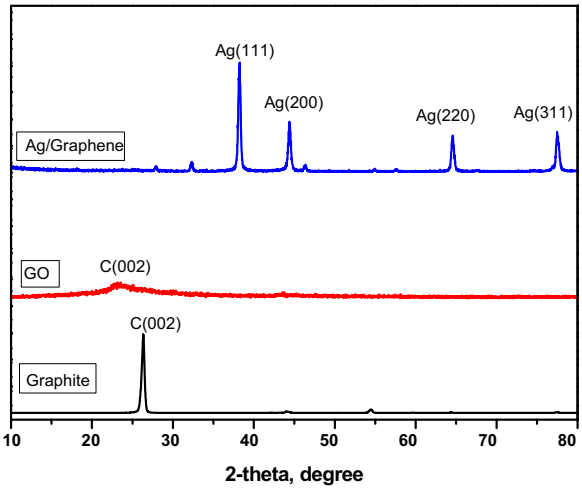

Fig. 4. XRD patterns of graphite, GO, and Ag/graphene.

believed that Ag atoms loaded on the surface of graphene sheets [21].

3.1.2. XRD

To further exhibit the microstructure of the as-prepared materials, the crystal structure was characterized by XRD. The XRD patterns of graphite, GO and Ag/graphene are recorded in Fig. 4. A strong C (0 0 2) peak at 26.34° and weak peak at 54° were shown in the patterns of raw graphite, and they were attributed to the reflection of a graphite structure of a carbon material. High purity graphite was used for the preparation of the Ag/graphene. For GO, the C (0 0 2) peak was also observed in its XRD patterns. But the broadness of the peak between 21° and 27° was ascribed to the oxygen-containing groups and inserted H_2O molecules. Amount of sp^2 carbons were replaced by these oxygen-containing groups, so the long-range order structure of carbon was destroyed. However, the Ag/graphene samples exhibited four reflection peaks, which can be indexed to Ag (1 1 1), Ag (2 0 0), Ag (2 2 0), and Ag (3 1 1) diffractions [22]. The crystallite size of the Ag particles supported graphene was calculated to be about 8 nm based on Scherrer's equation. In addition, there were no peaks of graphene detected, it could be speculated that Ag particles on the surface of graphene can inhibit the re-assembly of graphene layers. The exposed Ag active sites could benefit the adsorption.

3.1.3. TEM

To further characterize the microstructural morphology of the as-prepared samples, TEM was used and the results are shown in Fig. 5. TEM images of graphite, GO and Ag/GO were illustrated. As shown in Fig. 5(a), the flakes of raw graphite were thick and large, even though the sample was pretreated under ultrasonication. The typical TEM image of GO in Fig. 5(b), large sheets of carbon were observed on the top of grip. Almost all the carbon sheets were separated from each other. Fig. 5(c) and (d) showed the images of Ag/graphene, obviously, some large silver particles with a size of about 8–10 nm nanometers were loaded on the surface of the graphene sheets. The results matched well with the result of XRD patterns. However, the surface of Ag/graphene was rougher than GO and its sheets were agglomerate to some extent. It could be the result of reduction effect by hydrazine hydrate [23].

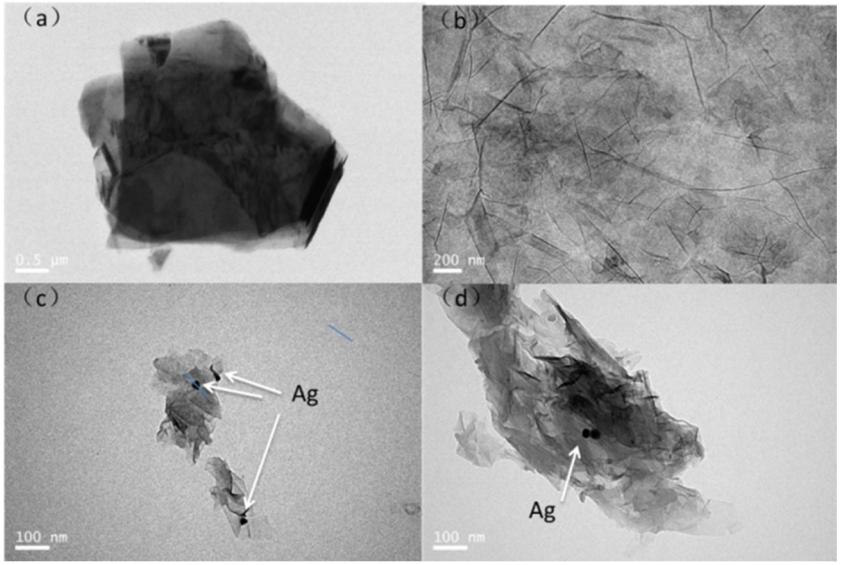

Fig. 5. TEM images graphite (a), GO (b), and Ag/graphene ((c) and (d)).

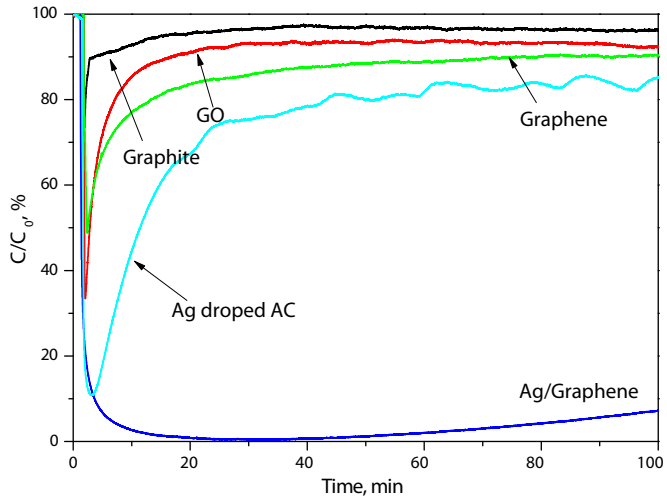

Fig. 6. Hg^0 adsorption performance of as-prepared samples at 25 °C.

3.2. Adsorption test

3.2.1. Hg^0 adsorption performance

In this work, the as-prepared samples were tested in a fixed-bed adsorption device. The graphite, GO, graphene, Ag/graphene and the Ag dropped AC were also tested for comparison. Mercury breakthrough curve at ambient temperature (25 °C) over these materials are presented in Fig. 6. It was found that the graphite had nearly no activity for the capture of Hg^0. Also, GO and graphene had very poor Hg^0 adsorption performance, the Hg^0 removal efficiency were lower than 20%. Ag/graphene showed the best Hg^0 adsorption performance, the Hg^0 removal efficiency was higher than 90% in 100 min. The Ag dropped AC was also tested for comparison, the result showed that Hg^0 removal efficiency was as low as 20% in 100 min. Ag/graphene had better performance than Ag dropped AC at this low temperature. The penetrable adsorption capability could get about 4.2 mg/g.

The Ag/graphene sorbent had the best performance for Hg^0 adsorption. As shown in Table 1, the BET surface areas of graphite, GO, graphene, Ag doped AC and Ag/graphene are given. The low activity for Hg^0 capture over graphite and GO could ascribed to the small surface area, the surface area of graphite and GO were 6.7 and 8.9 m^2/g, respectively. Graphene has the largest surface area (432 m^2/g), but it has no active sites for Hg^0 adsorption. Although

Table 1
BET surface areas of samples (graphite, GO, graphene, Ag doped AC, and Ag/graphene).

Sample	Surface area (m^2/g)
Graphite	6.7
GO	8.9
Graphene	432
Ag doped AC	365
Ag/graphene	251

Ag doped AC also had high surface area (365 m^2/g), the porous structure of AC prevented the interaction between Hg^0 and Ag particles. The mechanism for Hg^0 capture by Ag/graphene was that mercury formed in amalgamation with silver [13,24]. Ag–Hg alloy was obtained on the surface of graphene. Ag nanoparticles were the main active sites for Hg^0. The large surface area of graphene provided enormous room for Hg^0 migration. Graphene acted as a good supporter for Ag particles.

3.2.2. Effect of temperature for Hg^0 capture

The effect of temperature on Hg^0 removal was tested and the results are presented in Fig. 7(a). It was obvious that Hg^0 adsorption capacity of Ag/graphene decreased when the temperature increased. The Hg^0 adsorption capacity in 100 min dropped from 2.4 to 0.6 mg/g when the temperature rised from 25 to 100 °C, respectively. The higher adsorption temperature was not benefit for the capture of Hg^0. Additionally, the Hg^0 removal efficiency of Ag/graphene dropped from 94% at 25 °C to 60% at 100 °C, respectively. The poor performance of the Ag/graphene at high temperature was attributed to the mercury amalgamation mechanism. The Ag–Hg alloy was formed on the surface of graphene sheets, which showed low thermostability [24]. Therefore, the Ag/graphene showed poor performance at high temperature.

3.2.3. Effect of different gas composition

The Ag/graphene composite was limited for usage at high temperature. Also, the composition of the simulated gas could make an effect on Hg^0 capture. In general, flue gases from coal-fired power plants and cement plants contain several acid gases including sulfur dioxide (SO_2) in the range from a few hundred to a few thousand parts per million (ppm); and nitrogen oxides (e.g., NO) in the range from 200 to 2000 ppm. SO_2 and NO gas molecules may compete with Hg^0 for the active sites based on the previous studies [11,25]. The sorbents lose part of their Hg^0 capacity due to the competitive adsorption [26]. Thus, O_2, SO_2, NO and their mixture were chosen

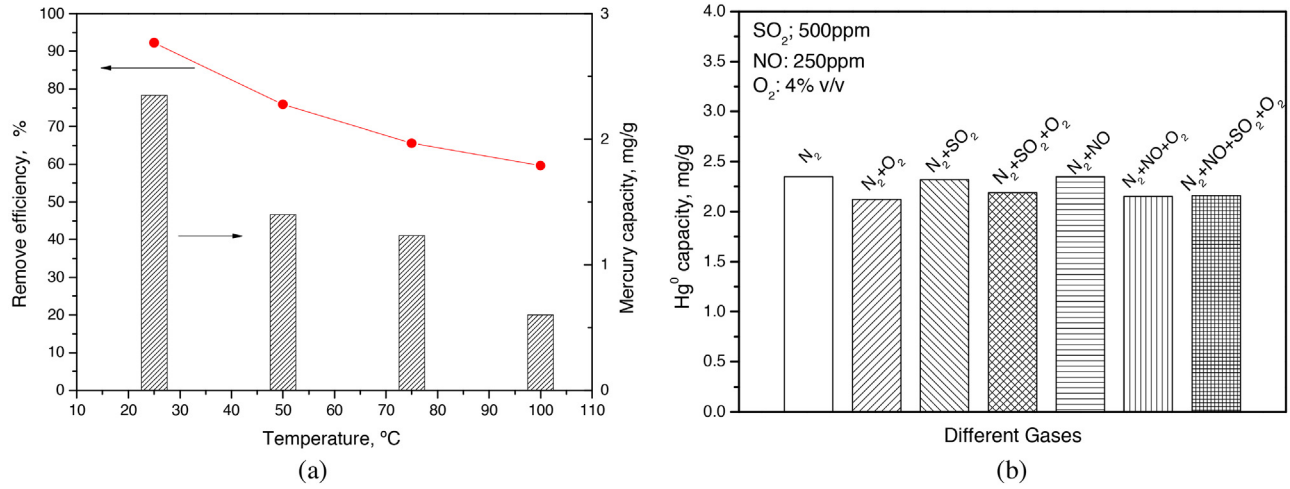

Fig. 7. (a) Effect of temperature on Ag/graphene; (b) effect of various gases on Ag/graphene.

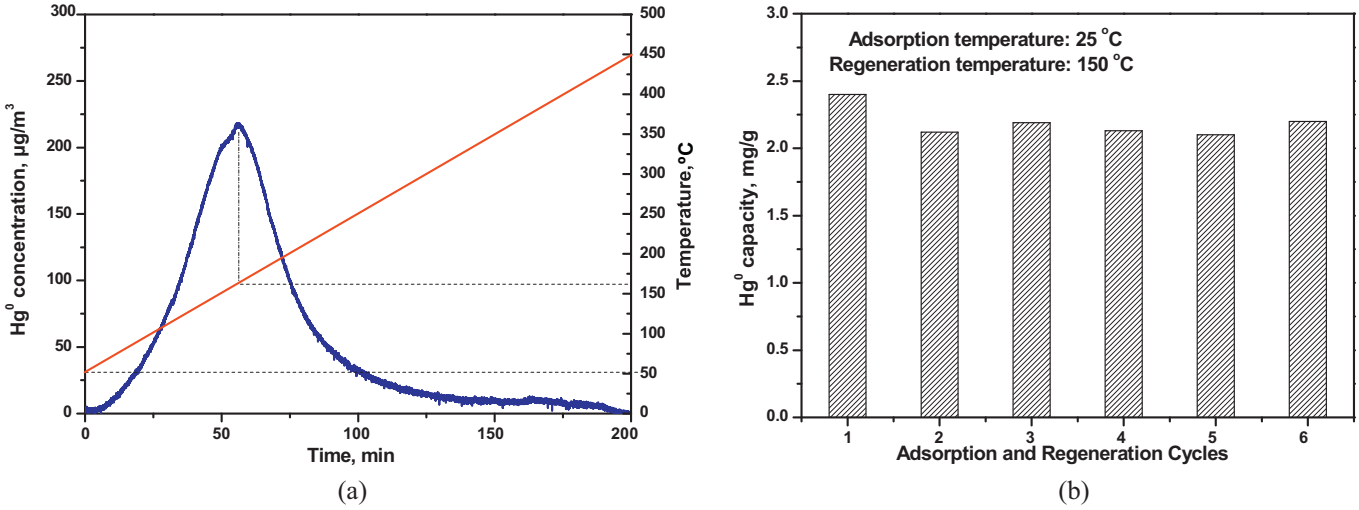

Fig. 8. (a) Hg-TPD; (b) Hg^0 capacities of Ag/graphene over different cycles of capture/regeneration.

for the test and the adsorption experiment was under 25 °C. As illustrated in Fig. 7(b), the results showed that SO_2 and NO have nearly no effects on Hg^0 removal, the Hg^0 capacity was almost the same as that in purity N_2. But the Hg^0 adsorption capacity dropped by 4% when O_2 existed. The Hg^0 capacity dropped about 5% compared the absence of O_2. It was believed that O_2 might inhibit the adsorption of Hg^0 to some extent. The reason was that Ag–Hg alloy could be easily affected by O_2 under ambient atmosphere, the surface of Ag during the amalgamation process could be occupied by oxygen atoms [24].

3.3. Sorbent recycling

One of the most important characters of one sorbent is its regenerability. Thermal regeneration was considered as an effective approach for mercury releasing from the surface of Ag/graphene composite. Hg-TPD method was built in our study to investigate the desorption performance of Hg^0 from the Ag/graphene sorbent. The Hg-TPD curves were collected under the heating rate of 2 °C min. As shown in Fig. 8(a), mercury began to release from the surface of Ag/graphene at the temperature of about 70 °C. A strong peak at 150 °C emerged during desorption process, the mercury release rate of Ag/graphene gets the highest. When the temperature higher than 400 °C, almost all the mercury evaporated from Ag/graphene. It was a rapid and efficient method to re-generate the sorbent because the low decomposition temperature of Ag–Hg alloy.

Hg^0 adsorption capacities of Ag/graphene composite after regeneration were also tested. As shown in Fig. 8(b), over six cycles of Hg^0 adsorption and regeneration, the capacity was keep almost the same to the first cycle of adsorption. Hg^0 capacity ranged from 2.1 to 2.4 mg/g compared with 2.4 mg/g in the first adsorption cycle. The result confirmed that Ag/graphene composite can be efficiently regenerated and reused. Ag/graphene was a potential sorbent for Hg^0 capture at low temperature.

4. Conclusion

In summary, Ag/graphene was successfully synthesized in a facile method based on the results of FRIR, XRD, and TEM. Ag particles were dispersed on the surface of graphene sheets. Graphene acted as a good supporter for Ag nanoparticles. Hg atoms transported on the surface of graphene and combined with Ag particles into Ag–Hg alloy. Ag/graphene exhibited excellent performance for Hg^0 capture at low temperature. Acid gases (NO, SO_2) almost had no effect on Hg^0 adsorption in the absence of O_2. Mercury as a resource could be collected from the Ag/graphene by a thermal regeneration method. The regeneration property makes it potential sorbent for Hg^0 control in the future.

Acknowledgments

This study was supported by the Major State Basic Research Development Program of China (973 Program, No. 2013CB430005), the National Natural Science Foundation of China (No. 50908145), and the National High-Tech R&D Program (863) of China (No. 2011AA060801).

References

[1] H. Yang, R.W. Battarbee, S.D. Turner, N.L. Rose, R.G. Derwent, G. Wu, R. Yang, Historical reconstruction of mercury pollution across the Tibetan Plateau using lake sediments, Environ. Sci. Technol. 44 (2010) 2918–2924.
[2] C.T. Driscoll, R.P. Mason, H.M. Chan, D.J. Jacob, N. Pirrone, Mercury as a global pollutant: sources, pathways, and effects, Environ. Sci. Technol. 47 (2013) 4967–4983.
[3] N. Pirrone, S. Cinnirella, X. Feng, R. Finkelman, H. Friedli, J. Leaner, R. Mason, A. Mukherjee, G. Stracher, D. Streets, Global mercury emissions to the atmosphere from anthropogenic and natural sources, Atmos. Chem. Phys. 10 (2010) 5951–5964.
[4] Y. Zheng, A.D. Jensen, C. Windelin, F. Jensen, Review of technologies for mercury removal from flue gas from cement production processes, Prog. Energy Combust. Sci. 38 (2012) 599–629.
[5] J.J. Rytuba, Mercury mine drainage and processes that control its environmental impact, Sci. Total Environ. 260 (2000) 57–71.
[6] M. Jang, S.M. Hong, J.K. Park, Characterization and recovery of mercury from spent fluorescent lamps, Waste Manage. 25 (2005) 5–14.
[7] N.C. Johnson, S. Manchester, L. Sarin, Y. Gao, I. Kulaots, R.H. Hurt, Mercury vapor release from broken compact fluorescent lamps and in situ capture by new nanomaterial sorbents, Environ. Sci. Technol. 42 (2008) 5772–5778.
[8] S. Liang, C. Zhang, Y. Wang, M. Xu, W. Liu, Virtual atmospheric mercury emission network in China, Environ. Sci. Technol. 48 (5) (2014) 2807–2815.
[9] Z. Tan, L. Sun, J. Xiang, H. Zeng, Z. Liu, S. Hu, J. Qiu, Gas-phase elemental mercury removal by novel carbon-based sorbents, Carbon 50 (2012) 362–371.
[10] A. Saha, D.N. Abram, K.P. Kuhl, J. Paradis, J.L. Crawford, E. Sasmaz, R. Chang, T.F. Jaramillo, J. Wilcox, An X-ray photoelectron spectroscopy study of surface changes on brominated and sulfur-treated activated carbon sorbents during mercury capture: performance of pellet versus fiber sorbents, Environ. Sci. Technol. 47 (2013) 13695–13701.
[11] A.A. Presto, E.J. Granite, Survey of catalysts for oxidation of mercury in flue gas, Environ. Sci. Technol. 40 (2006) 5601–5609.
[12] S. Manchester, X. Wang, I. Kulaots, Y. Gao, R.H. Hurt, High capacity mercury adsorption on freshly ozone-treated carbon surfaces, Carbon 46 (2008) 518–524.
[13] J. Dong, Z. Xu, S.M. Kuznicki, Mercury removal from flue gases by novel regenerable magnetic nanocomposite sorbents, Environ. Sci. Technol. 43 (2009) 3266–3271.

[14] G. Luo, H. Yao, M. Xu, X. Cui, W. Chen, R. Gupta, Z. Xu, Carbon nanotube–silver composite for mercury capture and analysis, Energy Fuels 24 (2009) 419–426.
[15] K.S. Novoselov, A.K. Geim, S. Morozov, D. Jiang, Y. Zhang, S. Dubonos, I. Grigorieva, A. Firsov, Electric field effect in atomically thin carbon films, Science 306 (2004) 666–669.
[16] V. Georgakilas, M. Otyepka, A.B. Bourlinos, V. Chandra, N. Kim, K.C. Kemp, P. Hobza, R. Zboril, K.S. Kim, Functionalization of graphene: covalent and non-covalent approaches, derivatives and applications, Chem. Rev. 112 (2012) 6156–6214.
[17] G. Zhao, J. Li, X. Ren, C. Chen, X. Wang, Few-layered graphene oxide nanosheets as superior sorbents for heavy metal ion pollution management, Environ. Sci. Technol. 45 (2011) 10454–10462.
[18] F. Guo, G. Silverberg, S. Bowers, S.-P. Kim, D. Datta, V. Shenoy, R.H. Hurt, Graphene-based environmental barriers, Environ. Sci. Technol. 46 (2012) 7717–7724.
[19] D. Li, M.B. Müller, S. Gilje, R.B. Kaner, G.G. Wallace, Processable aqueous dispersions of graphene nanosheets, Nat. Nanotechnol. 3 (2008) 101–105.
[20] A.V. Murugan, T. Muraliganth, A. Manthiram, Rapid, facile microwave-solvothermal synthesis of graphene nanosheets and their polyaniline nanocomposites for energy storage, Chem. Mater. 21 (2009) 5004–5006.
[21] R.V. Hull, L. Li, Y. Xing, C.C. Chusuei, Pt nanoparticle binding on functionalized multiwalled carbon nanotubes, Chem. Mater. 18 (2006) 1780–1788.
[22] J. Shen, M. Shi, N. Li, B. Yan, H. Ma, Y. Hu, M. Ye, Facile synthesis and application of Ag-chemically converted graphene nanocomposite, Nano Res. 3 (2010) 339–349.
[23] S. Stankovich, D.A. Dikin, R.D. Piner, K.A. Kohlhaas, A. Kleinhammes, Y. Jia, Y. Wu, S.T. Nguyen, R.S. Ruoff, Synthesis of graphene-based nanosheets via chemical reduction of exfoliated graphite oxide, Carbon 45 (2007) 1558–1565.
[24] R. Nowakowski, J. Pielaszek, R. Duś, Surface mediated Ag–Hg alloy formation under ambient and vacuum conditions – AFM and XRD investigations, Appl. Surf. Sci. 199 (2002) 40–51.
[25] J.H. Pavlish, E.A. Sondreal, M.D. Mann, E.S. Olson, K.C. Galbreath, D.L. Laudal, S.A. Benson, Status review of mercury control options for coal-fired power plants, Fuel Process. Technol. 82 (2003) 89–165.
[26] H. Yang, Z. Xu, M. Fan, A.E. Bland, R.R. Judkins, Adsorbents for capturing mercury in coal-fired boiler flue gas, J. Hazard. Mater. 146 (2007) 1–11.